C. R. Palevol 16 (2017) 533–544

Contents lists available at ScienceDirect

Comptes Rendus Palevol

www.sciencedirect.com

General Palaeontology

Does trabecular bone structure within the metacarpal heads of primates vary with hand posture?

La structure de l'os trabéculaire des têtes de métacarpiens de primates varie-t-elle avec la posture de la main ?

Habiba Chirchir[a,b,*], Angel Zeininger[c], Masato Nakatsukasa[d], Richard A. Ketcham[e], Brian G. Richmond[f,g]

[a] *Department of Biological Sciences, Marshall University, Huntington, USA*
[b] *Human Origins Program, National Museum of Natural History, Smithsonian Institution, Washington, USA*
[c] *Department of Evolutionary Anthropology, Duke University, Durham, USA*
[d] *Laboratory of Physical Anthropology, Graduate School of Science, Kyoto University, Kyoto, Japan*
[e] *Department of Geological Sciences, The University of Texas, Austin, USA*
[f] *Division of Anthropology, American Museum of Natural History, New York, USA*
[g] *Department of Human Evolution, Max Planck Institute for Evolutionary Anthropology, Leipzig, Germany*

ARTICLE INFO

Article history:
Received 8 August 2016
Accepted after revision 12 October 2016
Available online 6 December 2016

Handled by Roberto Macchiarelli and Clément Zanolli

Keywords:
Trabecular bone
BV/TV
Degree of anisotropy
Hand function
Bone volume

ABSTRACT

Reconstructing function from hominin fossils is complicated by disagreements over how to interpret primitively inherited, ape-like morphology. This has led to considerable research on aspects of skeletal morphology that may be sensitive to activity levels during life. We quantify trabecular bone morphology in three volumes of interest (dorsal, central, and palmar) in the third metacarpal heads of extant primates that differ in hand function: *Pan troglodytes*, *Pongo pygmaeus*, *Papio anubis*, and *Homo sapiens*. Results show that bone volume within third metacarpal heads generally matches expectations based on differences in function, providing quantitative support to previous studies. *Pongo* shows significantly low bone volume in the dorsal region of the metacarpal head. Humans show a similar pattern, as manipulative tasks mostly involve flexed and neutral metacarpo-phalangeal joint postures. In contrast, *Pan* and *Papio* have relatively high bone volume in dorsal and palmar regions, which are loaded during knuckle-walking/digitigrady and climbing, respectively. Regional variation in degree of anisotropy did not match predictions. Although trabecular morphology may improve behavioral inferences from fossils, more sophisticated quantitative strategies are needed to explore trabecular spatial distributions and their relationships to hand function.

Mots clés :
Os trabéculaire
BV/TV
Degré d'anisotropie
Fonction de la main
Volume osseux

RÉSUMÉ

Reconstruire la fonction à partir de fossiles homininés est une tâche compliquée par les désaccords concernant l'interprétation de la morphologie primitive des grands singes. Ceci a conduit à de nombreuses recherches sur différents aspects de la morphologie du squelette, qui pourraient être sensibles aux niveaux d'activité durant la vie d'un individu. Nous quantifions ici la morphologie de l'os trabéculaire selon trois volumes d'intérêt (dorsal, central

* Corresponding author. Department of Biological Sciences, Marshall University, Huntington, USA.
E-mail address: chirchir@marshall.edu (H. Chirchir).

http://dx.doi.org/10.1016/j.crpv.2016.10.002
1631-0683/

et palmaire) mesurés dans les têtes de métacarpiens de primates actuels qui diffèrent par la fonction de leurs mains : *Pan troglodytes*, *Pongo pygmaeus*, *Papio anubis* et *Homo sapiens*. Les résultats montrent que le volume osseux dans les têtes des troisièmes métacarpiens correspond généralement aux prévisions basées sur les différences de fonction, étayant de manière quantitative les précédentes études. *Pongo* montre un volume osseux significativement faible dans la région dorsale de la tête des métacarpiens. Les humains montrent un patron similaire, compatible avec le fait que les tâches de manipulation impliquent principalement les positions fléchies et neutres des articulations métacarpo-phalangiennes. À l'inverse, *Pan* et *Papio* ont un volume osseux relativement élevé dans les régions dorsale et palmaire, qui sont soumises à des contraintes lors de la locomotion sur les phalanges/digitigradie et de l'escalade. La variation régionale du degré d'anisotropie ne correspond pas à nos attentes. Bien que la morphologie trabéculaire puisse aider à améliorer les reconstructions comportementales des fossiles, des stratégies quantitatives plus sophistiquées sont nécessaires pour explorer la distribution spatiale trabéculaire et sa relation avec la fonction de la main.

> The reconstruction of postural and locomotor modes from skeletal remains is among the major topics of the paleoanthropological research, notably in the case of the earliest representatives of the hominin lineage whose behaviour is still a matter of discussion.
>
> Puymerail, 2013, p. 224

1. Introduction

Reconstructing behavior in early hominins has proven to be particularly challenging because of disagreements over how to interpret primitive morphology retained from earlier ancestors. For example, debate persists over when early hominins ceased arboreal behavior while still retaining some of the morphology associated with arboreality. Based on available data and methods, some researchers have interpreted the coexistence of primitive and derived characters in early hominins to indicate that they not only were bipeds on the ground, but also climbed trees (e.g., Deloison, 1985, 1997; Duncan et al., 1994; Green and Alemseged, 2012; Green et al., 2007; Jungers, 1982; Richmond, 2003; Richmond and Hatala, 2013; Schmitt, 2003; Spoor et al., 1994; Stern, 2000; Stern and Susman, 1983; Susman et al., 1984). The other interpretation is that derived morphologies indicate that arboreal climbing was severely compromised and the retention of primitive characters was unrelated to their behavior (e.g., Haile-Selassie et al., 2010; Latimer, 1991; Latimer and Lovejoy, 1990; Ward, 2002; Ward et al., 2011).

Difficulties in reconstructing function are not limited to issues concerning primitive and derived morphology. Many fossil taxa have morphology that is not present in any living species, making it difficult to examine the morphology's functional significance because it is not possible to experimentally examine the functional anatomy in living taxa (Lauder, 1995). For example, stone tool replication experiments by human subjects cannot fully take into account the mosaic and unique morphology in early hominin taxa (Susman, 1998).

However, this does not diminish the importance of replication experiments. They allow us to examine the biomechanical factors involved in particular functions, such as muscle recruitment involved in various grips and activities (Hamrick et al., 1998; Marzke et al., 1998), and the roles of anatomical regions in a particular function, such as thumb and finger positions and pressures during tool making (Marzke, 1997; Williams et al., 2012). Experimentation can also take advantage of natural variation to examine its effects on a function, such as digit length on muscle force during grip (Rolian et al., 2011). Additionally, anatomy can also be experimentally manipulated to examine its effects, such as the role of wrist mobility in generating force and accuracy during stone tool making (Williams et al., 2014) and the role of arm mobility in throwing force and accuracy (Roach and Lieberman, 2014; Roach et al., 2013). Most importantly, experimental and comparative studies generate more informed hypotheses about functional morphology and the behavior of extinct taxa.

So how can hypotheses about behavior in extinct taxa be tested? The best evidence comes from direct indications of past behavior, such as trace fossils (e.g., Hatala et al., 2016a, b), dietary traces (e.g., Henry et al., 2012), and skeletal anatomy that is sensitive to activity during life (e.g., Kivell, 2016; Ruff et al., 2006). The last approach is particularly relevant to examining postcranial functional morphology.

The relationship between mechanical loading and bone morphology (in both cortical and trabecular bone) is complex. There have been many studies investigating this relationship in long bone diaphyses (e.g., Demes and Jungers, 1993; Ruff et al., 1993, 2015; Runestad, 1997; Stock and Pfeiffer, 2001; Shaw and Stock, 2009; Trinkaus and Ruff, 1989a, b). Improved imaging technology has led to more intensive research on the morphology of trabecular bone (e.g., Barak et al., 2013; Chirchir et al., 2015; Desilva and Devlin, 2012; Griffin et al., 2010a; Maga et al., 2006; Matarazzo, 2015; Ryan and Ketcham, 2002; Ryan and Walker, 2010; Scherf and Tilgner, 2009; Skinner et al., 2015) which provides information on joint loading that is distinct from and compliments data on diaphyseal loading.

Experimental studies have shown that trabecular bone volume fraction (BV/TV = bone volume/total volume) and thickness increase in response to elevated loading regimes,

while decreased loading results in reduced trabecular BV/TV and thickness (e.g., Barak et al., 2011; Hou et al., 1990; Iwamoto et al., 1999; Mosley and Lanyon, 1998; Sakata et al., 1999). Additionally, changes in load direction or joint angle induce changes in trabecular orientation (e.g., Pontzer et al., 2006). Similarly, some comparative studies of primates with stereotypical locomotor behaviors or joint postures tend to show predictable trabecular orientations, and regional bone mineral density or BV/TV (e.g., Ryan and Ketcham, 2002, 2005; Saparin et al., 2011; Tsegai et al., 2013; Zeininger et al., 2011). However, insignificant relationships between predicted loading and trabecular morphology (e.g., BV/TV, DA, bone mineral density) have been found among some taxa in some anatomical regions (e.g., Carlson et al., 2008; Chirchir, 2016; Fajardo et al., 2007; Groll et al., 1999; Ryan and Walker, 2010; Shaw and Ryan, 2012), suggesting that the relationship between predicted loading and morphology is complex.

A few studies have focused on interpreting locomotor behavior in the fossil record based on interpretation of trabecular architecture in a number of specific elements (e.g. Barak et al., 2013; Desilva and Devlin, 2012; Skinner et al., 2015; Su et al., 2013; Zeininger et al., 2016). These studies have identified some trabecular bone properties that distinguish the fossil taxa, which have been attributed to differences in locomotor repertoire or tool use, albeit in a limited number of elements and taxa. Therefore, investigating trabecular architecture provides a promising method for interpreting function from morphology (Kivell, 2016).

Our study aims to build on this body of research by investigating trabecular bone architecture in the third metacarpal heads of catarrhines in order to understand the relationship between habitual hand postures and trabecular bone morphology. Previous research on hominoid metacarpals has found results that warrant further investigation. Zeininger et al. (2011) examined histological sections of third metacarpal heads in sagittal profile. They found that a measure of bone mineral density varied in predictable ways; for example, mineral density was significantly lower in the dorsal and palmar regions of chimpanzee metacarpal heads where joint stresses would be greatest during knuckle-walking and climbing hand postures. Orangutan and human metacarpal heads showed significantly different patterns. Using the same biomechanical models, Tsegai et al. (2013) examined trabecular structure in hominoid third metacarpal heads. Their results show that throughout the metacarpal heads BV/TV (bone volume/total volume), DA (degree of anisotropy), and trabecular thickness varied significantly among some taxa, but many comparisons did not show the expected significant differences (e.g., DA between *Pongo* and most of the African apes, contrary to predictions between suspensory and knuckle-walking behaviors). Visual comparisons suggest that suspensory and knuckle-walking taxa differ in the locations of greatest BV/TV and stiffness, but statistical comparisons were not available.

In this study, we aim to independently test Zeininger et al.'s (2011) and Tsegai et al.'s (2013) hypotheses that trabecular structure varies in predictable ways across regions of the metacarpal head, and that those patterns differ between taxa with different locomotor strategies. Expanding upon Tsegai et al.'s (2013) analysis based on selecting a single volume of interest in the center of the third metacarpal head, we selected three regions of the metacarpal head in the mid-sagittal plane – dorsal, central, and palmar regions – to examine whether they vary in a predictable manner with hand postures during locomotion in extant hominoids and baboons. We hypothesize that BV/TV and DA will reflect degree and direction of mechanical loading based on hand use. BV/TV has been shown to respond to the magnitude of loading, with increased magnitude associated with a high BV/TV (e.g., Courteix et al., 1998; Rubin and Lanyon, 1982). DA is a material property that represents the overall directionality of trabecular struts. Stereotypical loading patterns are associated with a relatively high DA (e.g., Fajardo and Müller, 2001; Huiskes et al., 2000; Ryan and Ketcham, 2005). As such, DA and BV/TV have been demonstrated to be good predictors of mechanical loading (e.g., Ding et al., 2002).

1.1. Predictions of trabecular bone morphology based on hand function in three regions of the third metacarpal head

The frequencies of various positional behaviors and the precise hand kinematics during locomotion, especially in the wild, among primate taxa are not well characterized and need further research. However, based on major differences in hand kinematics, we make several predictions of the regions of the metacarpo-phalangeal (MP) joint that habitually experience the greatest joint reaction forces (Tsegai et al., 2013; Zeininger et al., 2011).

Prediction 1. During knuckle-walking, chimpanzees use their digits in a flexed position to support body weight while the metacarpals are extended at the metacarpophalangeal joints (Jenkins and Fleagle, 1975; Tuttle, 1967) and the dorsal surface of the intermediate phalanges make contact with the substrate (Wunderlich and Jungers, 2009). Joint reaction forces are transmitted to the dorsal region of the metacarpal head during knuckle-walking (Fig. 1a), being highest in the 3rd and 4th metacarpals which absorb high compressive forces (Wunderlich and Jungers, 2009). This increased loading dorsally is thought to explain the mediolaterally expanded dorsal articular surface of the metacarpal head as a way to mediate joint reaction forces (Whitehead, 1993). Furthermore, chimpanzee third metacarpals have a dorsal ridge related to the degree of loading at the MP joint (Inouye, 1990). In addition to knuckle-walking, during arboreal locomotion, chimpanzees employ the suspensory transverse hook grip and the suspensory diagonal hook grip (Marzke and Wullstein, 1996), which involves variable flexion of MP joints (Fig. 1b). In this position, the palmar and palmar-distal surfaces of the metacarpal head experience the greatest joint loads. Thus, we predict that in chimpanzees, BV/TV and DA will be relatively similar in the dorsal and palmar regions of the third metacarpal head, both of which are predicted to be greater than in the central region due to greater loading during knuckle-walking and climbing.

Prediction 2. Orangutans engage in a considerable amount of suspensory postures and locomotion, and they rarely engage in behaviors that involve extended MP joints

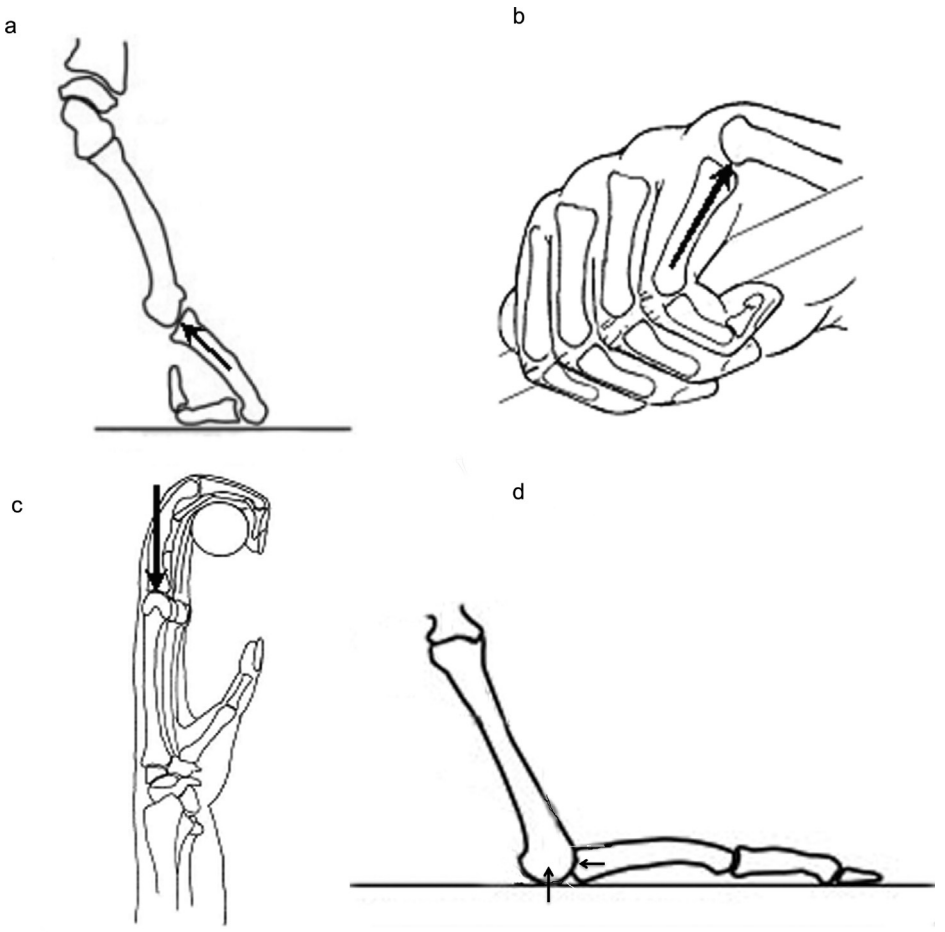

Fig. 1. Illustrations adapted from Richmond and Strait (2000) and Zeininger et al. (2011). a: diagram depicting direction of joint reaction force in an extended chimpanzee metacarpo-phalangeal joint with greater strain on the dorsal region; b: illustration of a flexed metacarpo-phalangeal joint posture (power grip) used by chimpanzees and orangutans during climbing as well as by humans during manipulation and carrying; c: direction of force in a metacarpo-phalangeal joint in orangutans with greater strain on the central regions; d: depiction of joint reaction force in a baboon during a digitigrade posture with most strain on the dorsal and central region.

Fig. 1. Illustrations adaptées d'après Richmond et Strait (2000) et Zeininger et al. (2011). a : diagramme illustrant la direction de la force de réaction de l'articulation dans une articulation métacarpo-phalangienne de chimpanzé en extension, avec une plus grande pression au niveau de la région dorsale ; b : illustration d'une articulation métacarpo-phalangienne en position fléchie (prise de force) chez le chimpanzé et l'orang-outan durant les phases d'escalade, ainsi que chez l'homme pendant la manipulation et le transport ; c : direction de la force dans une articulation métacarpo-phalangienne d'un orang-outan, avec une plus grande tension dans les régions centrales ; d : représentation de la force de réaction de l'articulation chez un babouin lors de la posture digitigrade, avec la plupart des tensions dans les régions dorsale et centrale.

(e.g., Cant, 1985; Thorpe and Crompton, 2006; Tuttle, 1967; Whitehead, 1993). They employ various hook grips and flexed finger postures during suspension and climbing. As the digits support body weight the palmar and central regions of the metacarpal head are thought to experience high joint forces (Fig. 1c). Therefore, we predict that in orangutans, the palmar and central regions will have relatively high BV/TV and DA compared to the dorsal region.

Prediction 3. Baboons walk on the ground using a digitigrade hand posture, with body weight supported by the metacarpal heads and phalanges (Hildebrand, 1988; Patel, 2010; Whitehead, 1993). During digitigrady, the distal region of the metacarpal head experiences substrate reaction forces while the dorsal region of the metacarpal head experiences MP joint reaction forces (Fig. 1d). However, at faster speeds, baboons adopt more palmigrade hand postures (Patel, 2010; Patel and Wunderlich, 2010); as the hands shift from digitigrade to palmigrade, the MP joint reaction force moves from the dorsal to the central region, and the substrate reaction force moves from central to palmar. Joint reaction forces at the MP joint are typically much higher than the substrate reaction forces (Cooney and Chao, 1977; Preuschoft, 1973; Richmond, 2007). Consequently, in baboons, we predict that there will be greater BV/TV and DA in the central and dorsal regions compared to the palmar regions of the metacarpal head.

Prediction 4. Humans use their hands in a variety of non-stereotypical ways, with actions ranging from very fine finger manipulations (e.g., precision grip) such as knitting to more generalized use such as holding tools (e.g., power grip; Fig. 1b). Some of these hand postures involve MP joint flexion while others do not (Marzke, 1997; Napier, 1993). Therefore, we predict that compared to all other taxa, humans will show the lowest DA because of

Table 1
Categories of hand function in the taxa investigated.
Tableau 1
Catégories des fonctions de la main chez les taxons étudiés.

Taxon	Sample size (n)	Hand function/locomotor behavior
Pan troglodytes	10	Knuckle-walking, vertical climbing
Pongo pygmaeus	10	Suspension, climbing
Papio anubis	9	Digitigrady, palmigrady
Homo sapiens	10	Manipulation

generally non-stereotypical hand use, and will have relatively similar and lower BV/TV throughout all regions than seen in other primates as has been reported elsewhere (Chirchir et al., 2015; Tsegai et al., 2013; Zeininger et al., 2011).

2. Materials and methods

We investigated a sample of 39 third metacarpal heads of four higher primate taxa: *Homo sapiens* ($n = 10$), *Pan troglodytes* ($n = 10$), *Pongo pygmaeus* ($n = 10$), and *Papio anubis* ($n = 9$) (Table 1). The non-human samples are wild collected and the modern humans were drawn from the Terry collection (late 19th century and early 20th century working class Americans). All specimens are housed at the National Museum of Natural History (NMNH), Smithsonian Institution, Washington. Following previous studies (Tsegai et al., 2013; Zeininger et al., 2011), third metacarpals were selected because their central position in the hand buffers them from mediolaterally-directed forces and consistently involves them in bearing weight during locomotion (e.g., Patel and Wunderlich, 2010; Wunderlich and Jungers, 2009). The sample consists of adult male and female individuals. However, sexually variable factors that may impact bone growth and development are not considered in this study and consequently data from both sexes are pooled. Specimens were scanned at two facilities. Metacarpals of three chimpanzees and three orangutans were scanned at the University of Texas at Austin's High-resolution X-ray CT (HRXCT) facility at 25 μm resolution while the remainder of the samples were scanned at the NMNH using a Stratec XCT Research SA CT (pQCT) scanner, at a 50-μm resolution. Although the two instruments are not the same, both were scanned at relatively high resolution and previous research using different scanning equipment has shown a good relationship between different scanning equipment (e.g., Chirchir et al., 2015). Lazenby et al. (2008) reported bilateral asymmetry in trabecular BV/TV in the hand. Here, we selected bones from the right hand when available (*P. troglodytes* all right side, *H. sapiens*; lefts = 1 and rights = 9; *P. pygmaeus*; lefts = 2, rights = 8; *P. anubis*; lefts = 1, rights = 8).

The program Quant3D (Ryan and Ketcham, 2002) was used to analyze trabecular bone structure. This program quantifies 3D properties of interest, including BV/TV and DA. The program allows the user to specify the size and location of a spherical volume of interest (VOI) within which trabecular properties are quantified.

In order to compare trabecular properties in the metacarpal head, we partitioned it into three regions: dorsal, central, and palmar VOIs (Fig. 2). We used spherical VOIs because the corners of cubic VOIs may bias the measurement of directionality (Ketcham and Ryan, 2004). VOIs were placed along the midline of the dorso-palmar axis of the joint surface. Utmost care was taken to avoid sampling the surrounding cortical bone at the joint surface. We selected a VOI size that was as large as possible without intersecting any cortical bone in any of the three regions in any of the samples. VOI size was determined to be the largest diameter that could fit within all three regions in a given bone. VOI size remained constant across regions within a specimen, so the smallest region determined the maximum size limit. While there are legitimate questions concerning how to best scale VOIs in studies comparing different species (Fajardo and Müller, 2001; Griffin et al., 2010a; Kivell et al., 2011; Lazenby et al., 2011), these issues have little impact in this study because the main comparisons are made within, rather than between, species.

Although our regional sampling strategy resulted in some overlap in VOIs, the spherical shape of the VOIs restricted overlap to very small proportions of the total volume. Slight overlap is preferable to making the VOIs so small that they do not adequately represent the structure of the joint regions. Within each VOI, bone was segmented using the FWHM (Full width/half maximum) threshold method (Trussell, 1979).

DA was measured using star volume distribution, which measures trabecular bone orientation by repeatedly sampling bone within the VOI and recording the lengths in all directions from the selected points within the bone to the bone-air interface (Ryan and Ketcham, 2002; Ryan and Krovitz, 2006). This was measured 2049 times, at 2000 random points as programmed in Quant3D. Eigenvalues were calculated based on the resulting orientation distributions. DA is calculated as the ratio of the primary eigenvalue over the tertiary eigenvalue, as a measure of the strength of orientation in the primary direction of the strength in the weakest perpendicular plane (Ryan and Ketcham, 2002). We performed Kruskal–Wallis tests with Nemenyi tests using R v.3.2.4 (2016) to test for significance across VOIs for each trabecular bone property within a taxon.

3. Results

Means and standard deviations of BV/TV and DA in each taxon and VOI are reported in Table 2. Within chimpanzee third metacarpal heads, although the central VOI exhibited the greatest mean BV/TV (Table 2), none of the VOIs were significantly different from one another (Table 3, Fig. 3a). Similarly, DA also did not differ significantly across the three VOIs in chimpanzees (Table 3, Fig. 3b). Orangutan third metacarpal heads exhibited significantly greater BV/TV in the palmar VOI than in the dorsal VOI, and significantly greater BV/TV in the central than the dorsal VOI ($P < 0.05$; Table 3, Fig. 4a). DA in the orangutan third metacarpal heads did not differ significantly among regions (Table 3, Fig. 4b).

In the baboon metacarpal heads, the observed BV/TV was not significantly different across the three VOIs (Fig. 5a,

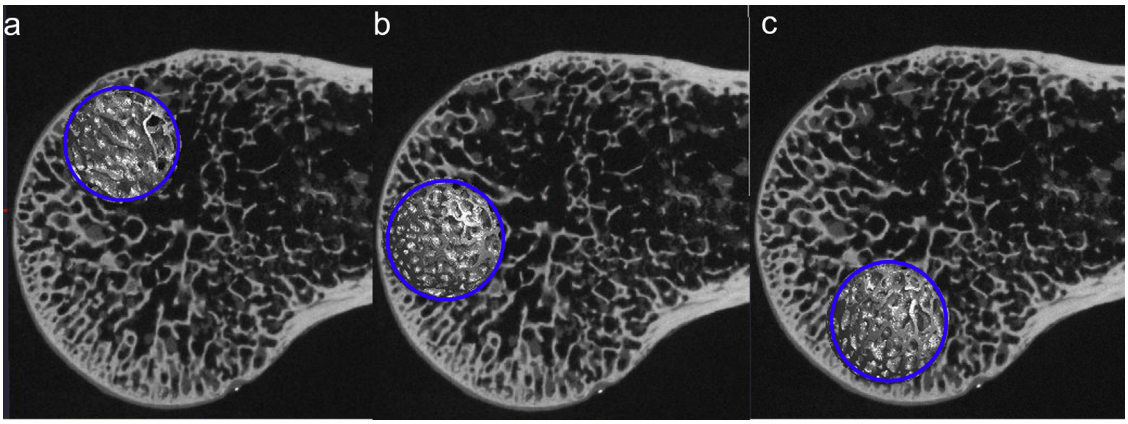

Fig. 2. Mid-sagittal cross-section of an orangutan third metacarpal head showing VOIs sampled (a) dorsal, (b) central, (c) palmar.
Fig. 2. Coupe transversale dans le plan sagittal médian de la tête d'un troisième métacarpien montrant les VOIs échantillonnés (a) dorsal, (b) central, (c) palmaire.

Table 2
Summary of means and standard deviations of BV/TV and DA in all species and all regions investigated.
Tableau 2
Résumé des moyennes et écarts-types de BV/TV et DA pour toutes les espèces et toutes les régions étudiées.

VOI	Taxon	*n*	BV/TV		DA	
			Mean	SD	Mean	SD
Dorsal	*H. sapiens*	10	0.08	0.04	3.09	1.05
	P. troglodytes	10	0.24	0.08	3.36	1.01
	P. pygmaeus	10	0.14	0.05	3.98	1.03
	P. anubis	9	0.23	0.07	5.32	2.15
Central	*H. sapiens*	10	0.13	0.04	2.68	0.58
	P. troglodytes	10	0.28	0.08	3.01	0.49
	P. pygmaeus	10	0.28	0.06	3.49	0.84
	P. anubis	9	0.23	0.06	5.21	2.16
Palmar	*H. sapiens*	10	0.12	0.03	2.72	0.78
	P. troglodytes	10	0.24	0.08	3.13	1.07
	P. pygmaeus	10	0.29	0.06	3.49	0.34
	P. anubis	9	0.22	0.05	4.05	1.62

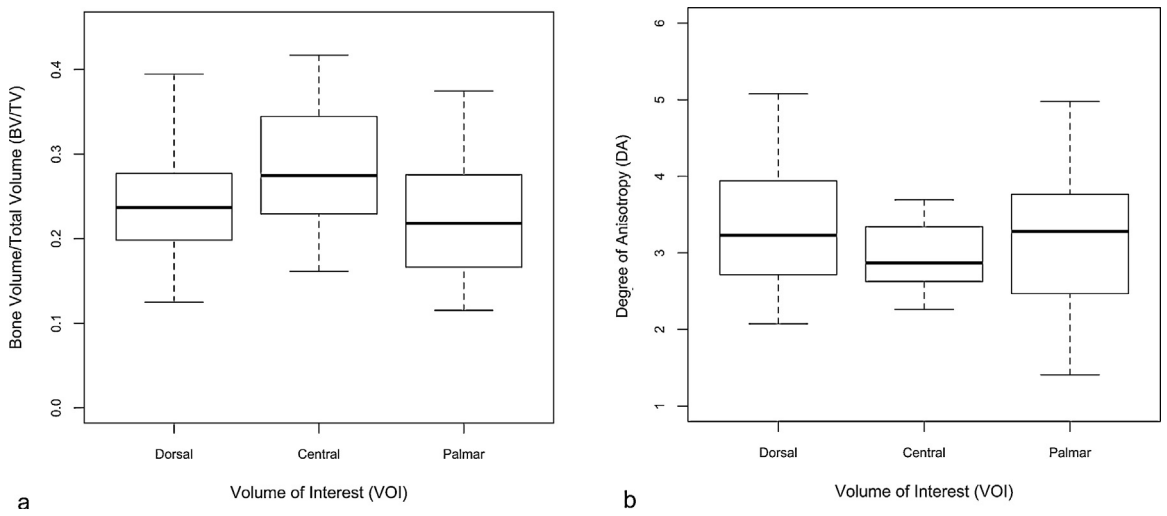

Fig. 3. Boxplots of (a) BV/TV and (b) DA in chimpanzees in all VOIs. In each boxplot, the central bold line shows the median, the box shows the interquartile range (25% and 75% values), and the whiskers show the values within 1.5 times the interqaurtile range above and below the box.
Fig. 3. Diagrammes en boîtes à moustaches de (a) BV/TV et (b) DA chez les chimpanzés pour tous les VOIs. Dans chaque graphique, la ligne centrale épaisse montre la médiane, la boîte délimite les écarts interquartiles (valeurs à 25 % et 75 %) et les moustaches indiquent les valeurs de l'écart interquartile à 1,5 fois au-dessus et au-dessous de la boîte.

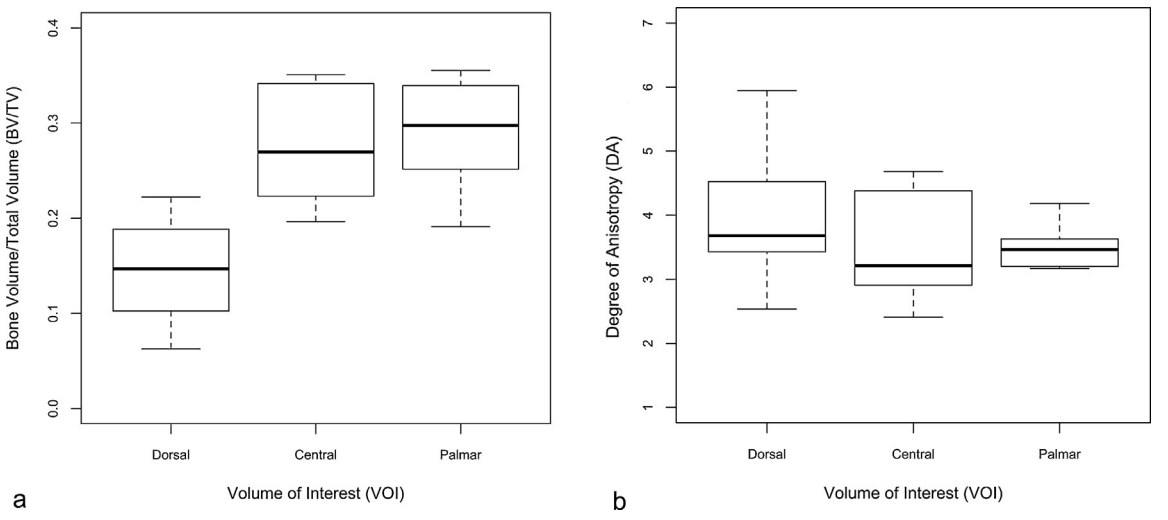

Fig. 4. Boxplots of (a) BV/TV and (b) DA in orangutans in all VOIs. See Fig. 3 for boxplot format details.

Fig. 4. Diagrammes en boîtes à moustaches de (a) BV/TV et (b) DA chez les orangs-outans pour tous les VOIs. Voir la Fig. 3 pour la lecture des graphiques.

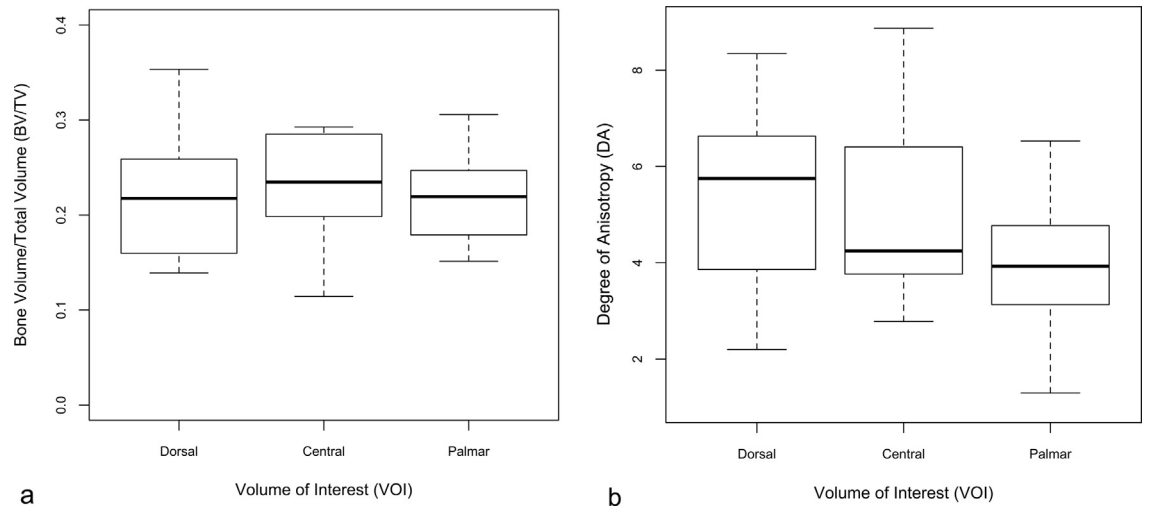

Fig. 5. Boxplots of (a) BV/TV and (b) DA in all VOIs in baboons. See Fig. 3 for boxplot format details.

Fig. 5. Diagrammes en boîtes à moustaches de (a) BV/TV et (b) DA chez les babouins pour tous les VOIs. Voir la Fig. 3 pour la lecture des graphiques.

Table 3). The pattern was somewhat similar to the chimpanzee BV/TV (Fig. 5a), with the greatest mean BV/TV in the central VOI but not significantly different from the other VOIs. Unlike BV/TV, the DA pattern in the baboon sample was different from the chimpanzee pattern. Although high DA values are observed in the dorsal region (Fig. 5b), the differences across the VOIs were not statistically significant (Table 3).

Lastly, in humans, the dorsal VOI had significantly lower BV/TV than the central VOI but not the palmar ($P < 0.05$; Table 3, Fig. 6a). There was no significant difference in DA across the three VOIs (Fig. 6b, Table 3). In comparison to other taxa, BV/TV was significantly lower in all VOIs compared with other taxa (Table 4), whereas DA was not significantly lower than other taxa except central VOI of *P. anubis* ($P < 0.05$).

4. Discussion

The results show that the distribution of trabecular bone volume (BV/TV) matches some of the predictions based on species-specific differences in habitual hand use, whereas the distribution of degree of anisotropy (DA) does not. The findings here show that habitual biomechanical loading has an influence on trabecular morphology consistent with reports by other researchers (e.g., Griffin et al., 2010a; Pontzer et al., 2006; Rafferty, 1998; Ryan and Ketcham, 2002; Tsegai et al., 2013), albeit not in both trabecular properties investigated.

The first prediction that chimpanzees have relatively similar BV/TV and DA in both palmar and dorsal regions of the third metacarpal head is supported by our findings. Specifically, there is no significant difference in either

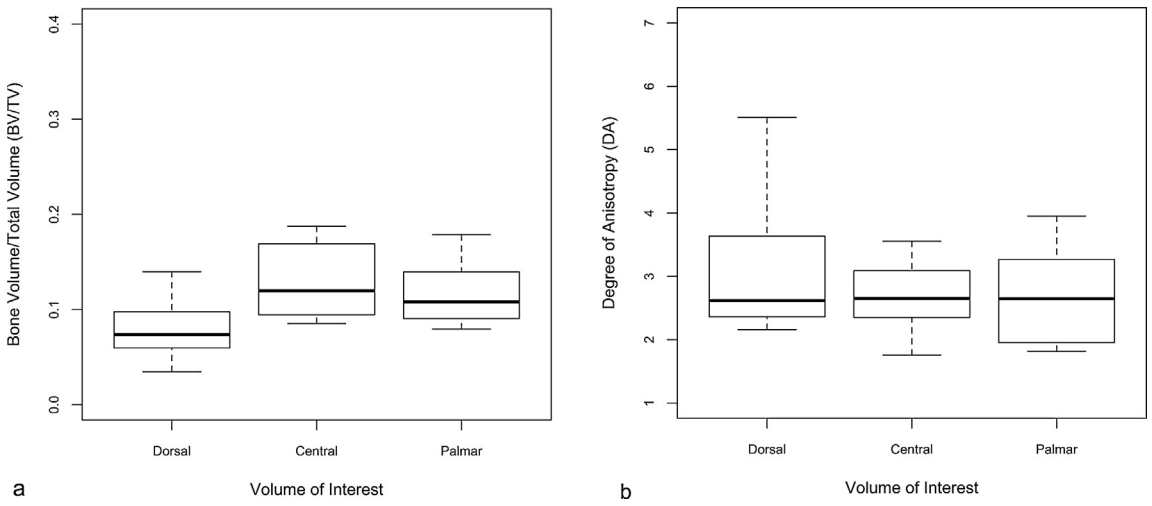

Fig. 6. Boxplots of (a) BV/TV and (b) DA in modern humans in all VOIs. See Fig. 3 for boxplot format details.
Fig. 6. Diagrammes en boites à moustaches de (a) BV/TV et (b) DA chez les humains pour tous les VOIs. Voir la Fig. 3 pour la lecture des graphiques.

Table 3
Kruskal–Wallis test with Nemenyi post-hoc tests across VOIs for each taxon. Significant differences ($P < 0.05$) between VOIs are shown in bold face.
Tableau 3
Tests de Kruskall–Wallis avec des tests post-hoc de Nemenvi entre VOIs pour chaque taxon. Les différences significatives ($p < 0{,}05$) entre les VOIs sont indiquées en gras.

Taxon	Dorsal vs. central VOI	Palmar vs. central VOI	Dorsal vs. palmar VOI
P. troglodytes			
BV/TV	0.53	0.4	0.97
DA	0.74	0.96	0.87
P. pygmaeus			
BV/TV	**0.001**	0.99	**0.007**
DA	0.56	0.98	0.73
P. anubis			
BV/TV	0.96	0.94	1
DA	0.99	0.58	0.54
H. sapiens			
BV/TV	**0.02**	0.71	0.13
DA	0.73	0.99	0.63

BV/TV or DA between the two regions in chimpanzees (Table 3). However, contrary to predictions, the central region is not significantly lower in BV/TV than the dorsal and palmar regions (Fig. 3a). This might be explained by the diversity in hand postures and positional behaviors among chimpanzees, which result in loading at the MP joint from a variety of postures. Specifically, knuckle-walking and flexed-joint hand postures during climbing could explain the high DA values in the dorsal and palmar VOIs, respectively. Perhaps the BV/TV in the central region remains high to keep the entire metacarpal head strong through the range of regularly used hand postures, including partly-flexed MP joints used in a variety of climbing grips (e.g., Fig. 1b and c). Chimpanzees engage in a variety of postures and locomotor behaviors in the trees (e.g., Carlson et al., 2006; Doran, 1993a, b). Predicting joint reaction forces distribution in the chimpanzee hand is complicated by factors, such as age changes in locomotion, body mass, and type and size of substrate (Doran, 1993a, b, 1997). However, chimpanzees spend ~84% of the time on the ground; during knuckle-walking, the MP joints are stereotypically loaded in extended postures and the second and third digits experience the greatest stresses (Wunderlich and Jungers, 2009). If trabecular bone is sensitive to differences in loading then, despite the highly flexible nature of hand use during locomotion, habitual behaviors as different as knuckle-walking and suspension should be detectable. If not, then it raises serious concerns about using trabecular structure to make behavioral inferences in the fossil record.

Zeininger et al. (2011) show that patterns of bone mineral density better match the hypothesis that knuckle-walking and climbing concentrate mechanically demanding loads on the dorsal and palmar regions. However, in that study (Zeininger et al., 2011), the lower bone mineral density (associated with elevated remodeling levels) were most pronounced in subchondral bone towards the margins of the joint. Similarly, Tsegai et al. (2013) report that the BV/TV values are especially high in the dorsal-most region and dorsal ridge. The VOIs selected here may not sample quite the same region (e.g., spherical VOIs cannot sample much trabecular bone very close to the joint surface).

Tsegai et al. (2013) also report that, compared to the dorsal region, BV/TV values appear to be lower in the palmar regions of their African ape samples, based on visual inspection of scaled color maps. Our results contrast slightly, in that the palmar VOIs in the chimpanzee sample are equivalent to the dorsal VOIs in BV/TV (Table 3, Fig. 3). Similarly, our results show equivalent DA values in those regions (i.e. the dorsal and palmar VOIs). The visualization maps in Tsegai et al. (2013) suggest a pattern of somewhat lower values in these regions. It would be valuable to follow up our and Tsegai et al.'s (2013) study with other strategies to quantify and statistically examine the distributions of trabecular characteristics. Our understanding of the link between trabecular morphology and behavior could be greatly improved with the development of more thorough

Table 4
P-values from Kruskal–Wallis tests with Nemenyi post-hoc test between *H. sapiens* and all other taxa (i.e. *P. troglodytes*, *P. pygmaeus*, and *P. anubis*), significant *P*-values are shown in bold face.
Tableau 4
Valeurs *p* des tests de Kruskal–Wallis avec des tests post-hoc de Nemenvi entre *H. sapiens* et les autres taxons (i.e. *P. troglodytes*, *P. pygmaeus* et *P. anubis*). Les valeurs de *p* significatives sont indiquées en gras.

	BV/TV			DA		
VOI	*P. troglodytes*	*P. pygmaeus*	*P. anubis*	*P. troglodytes*	*P. pygmaeus*	*P. anubis*
Dorsal	**<0.001**	**0.03**	**0.001**	0.88	0.055	0.351
Central	**0.007**	**0.06**	**<0.001**	0.79	0.19	**0.004**
Palmar	**0.007**	**0.017**	**<0.001**	0.74	0.084	0.311

quantitative strategies coupled with much more thorough documentation of behavior, such as hand postures used in natural settings that should be a high priority for future research (Richmond et al., 2016).

The second prediction that orangutans will have greater BV/TV and a high DA in the palmar and central regions compared to the dorsal region is partially supported by the results – the BV/TV values match expectations whereas the DA results do not. We found that there is significantly greater BV/TV in the palmar and central VOIs compared to the dorsal VOI (Fig. 4a, Tables 2 and 3). These results are consistent with the BV//TV color maps and stiffness maps reported in a different sample of orangutan third metacarpals (Tsegai et al., 2013), and with data showing lower bone mineral density in the palmar-distal regions (Zeininger et al., 2011). These results support the hypothesis that the dorsal portion of the orangutan metacarpal is not typically subjected to joint forces, as extended MP joint postures are not usually used during suspension and climbing. Suspensory taxa instead use highly flexed fingers when grasping relatively small supports, and neutral MP joint postures during hook grips (Cant, 1985; Sarmiento, 1988; Fig. 1c). Here, trabecular BV/TV shows a clear pattern related to habitual use.

Orangutan third metacarpal DA on the other hand, did not follow the predicted pattern. This demonstrates the complexity of interpreting DA. Experimental research finds no differences in DA between running and control mice in the hindlimb (e.g., Carlson et al., 2008). Additionally, Matarazzo (2015) found that when individual trabecular bone properties are examined in phalanges and metacarpal heads of primates, they do not fully reflect locomotor behavior. Thus, we suggest that the bone in the orangutan dorsal metacarpal head remains anisotropic with struts oriented towards the joint surface in order to resist the forces that occur, however infrequently.

Thirdly, the prediction that baboons will have the greatest BV/TV and DA on the dorsal and central regions is not well supported by our results because there were no significant differences across VOIs in either BV/TV or DA (Tables 3, Fig. 5a and b). The lack of difference suggests that the MP joint posture is not sufficiently stereotypical to leave a distinct trabecular pattern. For example, in human feet, the metatarsal heads have a striking pattern of increasing BV/TV and DA from plantar to dorsal that contrasts with the patterns in great ape metatarsal heads (Griffin et al., 2010a). Humans, of course, use their feet in far more stereotypical ways than do great apes, and humans walk and run with metatarsophalangeal joints that are more highly extended than those of bonobos, for example (Griffin et al., 2010b). Baboons use extended MP joints on the ground but shift to palmigrade postures with neutral MP joints at higher speeds (Patel, 2010). This, in combination with varying amounts of tree-climbing activities, such as sleeping and feeding (Altmann, 1974), which may explain the fairly consistent distribution of bone throughout the third metacarpal head.

Lastly, we predicted that modern humans would have low and relatively uniform BV/TV and low DA in all regions due to the non-stereotypical hand use and relatively low (non-locomotor) levels of force. Our results partially support this prediction. First, BV/TV in the dorsal VOI was significantly lower than the central but not palmar VOI (Table 3, Fig. 6a). Like orangutans, human hand functions typically involve little hyperextension at the MP joints. Human MP joints are used in neutral and flexed positions during carrying and manual manipulation (Goldfarb and Dovan, 2006; Marzke, 1997; Napier, 1993). In all regions, BV/TV was very low compared with the other taxa (Table 4, Fig. 6a), adding further support to research showing that low bone volume throughout the skeleton appeared very recently in human evolution (Chirchir et al., 2015), likely after abandoning a hunter-gatherer lifestyle (Ryan and Shaw, 2015). The low BV/TV throughout the third metacarpal head observed in this study are consistent with Tsegai et al.'s (2013) findings as well. Human DA was not significantly different from most taxa, suggesting that even with low BV/TV, trabecular bone is structured to resist loads.

In summary, the distribution of BV/TV within the third metacarpal head reflects species-specific differences in habitual joint loading. While some species show fewer differences among regions than predicted, all of the observed differences are consistent with hand function. In contrast, the spatial pattern of DA did not match predictions, and remained at similar levels in regions with high and low bone volume. This suggests that the spatial pattern of DA may be more informative in situations involving highly stereotypical loading, such as the distinct pattern of dorsally-increasing DA in the metatarsal heads of humans (Griffin et al., 2010a), who habitually hyperextend the toes during walking and running and do little else demanding with those joints. We also note that the principal orientations of anisotropic structure and variations in anisotropic

structure (e.g., rods, plates) can be informative (e.g., Ryan and Ketcham, 2002).

5. Conclusions

This study used a simple approach of examining three distinct regions within the epiphysis of a mobile joint. We suggest that it would be useful to develop more sophisticated approaches to statistically compare spatial patterns of trabecular structure. Also needed are data documenting function with finer resolution, such as hand postures used by primates in natural settings. Spatial analytical approaches together with finer-scale data on behavior will improve our abilities to understand the form-function relationship. This in turn will lead to more robust interpretations of the functional behavior of our long-extinct ancestors and relatives. Indeed with the development of improved quantification strategies, trabecular bone morphology holds promise of improving behavioral inferences in the fossil record.

Acknowledgments

We thank Roberto Macchiarelli and Clément Zanolli for the invitation to contribute to the *C. R. Palevol.* thematic issue titled "Hominin biomechanics, virtual anatomy and inner structural morphology: from head to toe. A tribute to Laurent Puymerail. We also thank David Hunt and Linda Gordon for providing access to the study samples, and two anonymous reviewers for their constructive suggestions. This research was supported by NSF DGE-0801634; NSF BCS-0521835, the Wenner–Gren Foundation's Wadsworth Fellowship and the Leakey Foundation's Baldwin Fellowship.

References

Altmann, S.A., 1974. Baboons, space, time, and energy. Am. Zool. 14, 221–248.
Barak, M.M., Lieberman, D.E., Hublin, J.-J., 2011. A Wolff in sheep's clothing: trabecular bone adaptation in response to changes in joint loading orientation. Bone 49, 1141–1151.
Barak, M.M., Lieberman, D.E., Raichlen, D., Pontzer, H., Warrener, A.G., Hublin, J.-J., 2013. Trabecular evidence for a human-like gait in *Australopithecus africanus*. PLoS One 8, e77687.
Cant, J.G.H., 1985. Locomotor and postural behavior of orang-utan (*Pongo pygmaeus*) in Borneo and Sumatra. Am. J. Phys. Anthropol. 66, 153 (abstract).
Carlson, K.J., Doran-Sheehy, D.M., Hunt, K.D., Nishida, T., Yamanaka, A., Boesch, C., 2006. Locomotor behavior and long bone morphology in individual free-ranging chimpanzees. J. Hum. Evol. 50, 394–404.
Carlson, K.J., Lublinsky, S., Judex, S., 2008. Do different locomotor modes during growth modulate trabecular architecture in the murine hind limb? Integr. Comp. Biol. 48, 385–393.
Chirchir, H., 2016. Limited trabecular bone density heterogeneity in the human skeleton. Anat. Res. Int. 9295383, 1–7.
Chirchir, H., Kivell, T.L., Ruff, C.B., Hublin, J.-J., Carlson, K.J., Zipfel, B., Richmond, B.G., 2015. Recent origin of low trabecular bone density in modern humans. Proc. Natl. Acad. Sci. U.S.A. 112, 366–371.
Cooney, W.P., Chao, E.Y., 1977. Biomechanical analysis of static forces in the thumb during hand function. J. Bone Joint Surg. 59, 27–36.
Courteix, D., Lespessailles, E., Loiseau, P.S., Obert, P., Germain, P., Benhamou, C.L., 1998. Effects of physical training on bone mineral density in prepubertal girls: a comparative study between impact-loading and non-impact-loading sports. Osteopor. Int. 8, 152–158.
Deloison, Y., 1985. Comparative study of calcanei of primates and *Pan–Australopithecus–Homo relationship*. In: Tobias, P.V. (Ed.), Hominid Evolution: Past, Present and Future. Alan R. Liss, Inc., New York, pp. 143–147.
Deloison, Y.M.-L., 1997. The foot bones from Hadar, Ethiopia and the Laetoli, Tanzania footprints. Locomotion of *A. afarensis*. Am. J. Phys. Anthropol Suppl. 24, 100 (abstract).
Demes, B., Jungers, W.L., 1993. Long bone cross-sectional dimensions, locomotor adaptations, and body size in prosimian primates. J. Hum. Evol. 25, 57–74.
Desilva, J.M., Devlin, M.J., 2012. A comparative study of the trabecular bony architecture of the talus in humans, non-human primates, and *Australopithecus*. J. Hum. Evol. 63, 536–551.
Ding, M., Odgaard, A., Danielsen, C.C., Hvid, I., 2002. Mutual associations among microstructural, physical and mechanical properties of human cancellous bone. J. Bone Joint Surg. 84-B, 900–907.
Doran, D.M., 1993a. Comparative locomotor behavior of chimpanzees and bonobos: the influence of morphology on locomotion. Am. J. Phys. Anthropol. 91, 83–98.
Doran, D.M., 1993b. Sex differences in adult chimpanzee positional behavior: the influence of body size on locomotion and posture. Am. J. Phys. Anthropol. 91, 99–115.
Doran, D.M., 1997. Ontogeny of locomotion in mountain gorillas and chimpanzees. J. Hum. Evol. 32, 323–344.
Duncan, A.S., Kappelman, J., Shapiro, L., 1994. Metatarsophalangeal joint function and positional behavior in *Australopithicus afarensis*. Am J. Phys. Anthropol. 93, 67–81.
Fajardo, R.J., Müller, R., 2001. Three-dimensional analysis of nonhuman primate trabecular architecture using micro-computed tomography. Am. J. Phys. Anthropol. 115, 327–336.
Fajardo, R.J., Müller, R., Ketcham, R.A., Colbert, M., 2007. Nonhuman anthropoid primate femoral neck trabecular architecture and its relationship to locomotor mode. Anat. Rec. 290, 422–436.
Goldfarb, C.A., Donan, T.T., 2006. Rheumatoid arthritis: silicone metacarpophalangeal joint arthroplasty indications, technique, and outcomes. Hand Clin. 22, 177–182.
Green, D.J., Alemseged, Z., 2012. *Australopithecus afarensis* scapular ontogeny, function, and the role of climbing in human evolution. Science 338, 514–517.
Green, D.J., Gordon, A.D., Richmond, B.G., 2007. Limb-size proportions in *Australopithecus afarensis* and *Australopithecus africanus*. J. Hum. Evol. 52, 187–200.
Griffin, N.L., D'Aout, K., Ryan, T.M., Richmond, B.G., Ketcham, R.A., Postnov, A., 2010a. Comparative forefoot trabecular bone architecture in extant hominids. J. Hum. Evol. 59, 202–213.
Griffin, N.L., D'Aout, K., Richmond, B.G., Gordon, A., Aerts, P., 2010b. Comparative in vivo forefoot kinematics of *Homo sapiens* and *Pan paniscus*. J. Hum. Evol. 59, 608–619.
Groll, O., Lochmüller, E.M., Bachmeier, M., Willnecker, J., Eckstein, F., 1999. Precision and intersite correlation of bone densitometry at the radius, tibia and femur with peripheral quantitative CT. Skeletal. Radiol. 12, 696–702.
Haile-Selassie, Y., Latimer, B.M., Alene, M., Deino, A.L., Gibert, L., Melillo, S.M., Saylor, B.Z., Scott, G.R., Lovejoy, C.O., 2010. An early *Australopithecus afarensis* postcranium from Woranso-Mille, Ethiopia. Proc. Natl. Acad. Sci. U.S.A. 107, 12121–12126.
Hamrick, M.W., Churchill, S.E., Schmitt, D., Hylander, W.L., 1998. EMG of the human *flexor pollicis longus* muscle: implications for the evolution of hominid tool use. J. Hum. Evol. 34, 123–136.
Hatala, K.G., Roach, N.T., Ostrofsky, K.R., Wunderlich, R.E., Dingwall, H.L., Villmoare, B.A., Green, D.J., Harris, J.W.K., Braun, D.R., Richmond, B.G., 2016a. Footprints reveal direct evidence of group behavior and locomotion in *Homo erectus*. Sci. Rep. 6, 28766.
Hatala, K.G., Wunderlich, R.E., Dingwall, H.L., Richmond, B.G., 2016b. Interpreting locomotor biomechanics from the morphology of human footprints. J. Hum. Evol. 90, 38–48.
Henry, A.G., Ungar, P.S., Passey, B.H., Sponheimer, M., Rossouw, L., Bamford, M., Sandberg, P., de Ruiter, D.J., Berger, L., 2012. The diet of *Australopithecus sediba*. Nature 487, 90–93.
Hildebrand, M., 1988. Analysis of vertebrate structure, 3rd ed. John Wiley and Sons, New York.
Hou, J.C-H., Salem, G.J., Zernicke, R.F., Barnard, J.R., 1990. Structural and mechanical adaptations of immature trabecular bone to strenuous exercise. Am. Phys. Soc. 69, 1309–1314.
Huiskes, R., Ruimerman, R., Harry van Lenthe, G., Janssen, J.D., 2000. Effects of mechanical forces on maintenance and adaptation of form in trabecular bone. Nature 405, 704–706.
Inouye, S.E., 1990. Variation in the presence and development of the dorsal ridge of the metacarpal head in African apes. Am. J. Phys. Anthropol. 81, 243 (abstract).

Iwamoto, J., Yeh, J.K., Aloia, J.F., 1999. Differential effect of treadmill exercise on three cancellous bone sites in the young growing rat. Bone 24, 163–169.
Jenkins Jr., F.A., Fleagle, J.G., 1975. Knuckle-walking and the functional anatomy of the wrists in living apes. In: Tuttle, R.H. (Ed.), Primate Functional Morphology and Evolution. Mouton Publisher, The Hague, pp. 213–227.
Jungers, W.L., 1982. Lucy's limbs: skeletal allometry and locomotion in *Australopithecus afarensis*. Nature 297, 676–678.
Ketcham, R.A., Ryan, T.M., 2004. Quantification and visualization of anisotropy in trabecular bone. J. Microsc. 213, 158–171.
Kivell, T.L., 2016. A review of trabecular bone functional adaptation: what have we learned from trabecular analyses in extant hominoids and what can we apply to fossils? J. Anat. 228, 569–594.
Kivell, T.L., Skinner, M.M., Lazenby, R., Hublin, J.-J., 2011. Methodological considerations for analyzing trabecular architecture: an example from the primate hand. J. Anat. 218, 209–225.
Latimer, B.M., 1991. Locomotor adaptations in *Australopithecus afarensis*: the issue of arboreality. In: Coppens, Y., Senut, B. (Eds.), Origine(s) de la Bipédie chez les Hominidés. Éditions du CNRS, Paris, pp. 169–176.
Latimer, B.M., Lovejoy, C.O., 1990. Hallucal tarsometatarsal joint in *Australopithecus afarensis*. Am. J. Phys. Anthropol. 82, 125–133.
Lauder, G.V., 1995. On the inference of function from structure. In: Thompson, J.J. (Ed.), Functional Morphology in Vertebrate Paleontology. Cambridge University Press, Cambridge, pp. 1–18.
Lazenby, R.A., Cooper, D.M., Angus, S., Hallgrimsson, B., 2008. Articular constraint, handedness, and directional asymmetry in the human second metacarpal. J. Hum. Evol. 54, 875–885.
Lazenby, R.A., Skinner, M.M., Kivell, T.L., Hublin, J.-J., 2011. Scaling VOI size in 3D μCT studies of trabecular bone: a test of the over-sampling hypothesis. Am. J. Phys. Anthropol. 144, 196–203.
Maga, M., Kappelman, J., Ryan, T.M., Ketcham, R.A., 2006. Preliminary observations on the calcaneal trabecular microarchitecture of extant large-bodied hominoids. Am. J. Phys. Anthropol. 129, 410–417.
Marzke, M.W., 1997. Precision grips, hand morphology, and tools. Am. J. Phys. Anthropol. 102, 91–110.
Marzke, M.W., Wullstein, K.L., 1996. Chimpanzee and human grips: a new classification with a focus on evolutionary morphology. Int. J. Primatol. 17, 117–139.
Marzke, M.W., Toth, N., Schick, K., Reece, S., Steinberg, B., Hunt, K., Linscheid, R.L., An, K.-N., 1998. EMG study of hand muscle recruitment during hard hammer percussion manufacture of Oldowan tools. Am. J. Phys. Anthropol. 105, 315–332.
Matarazzo, S.A., 2015. Trabecular architecture of the manual elements reflects locomotor patterns in primates. PLoS One 10, e0120436.
Mosley, J.R., Lanyon, L.E., 1998. Strain rate as a controlling influence on adaptive modeling in response to dynamic loading of the ulna in growing male rats. Bone 23, 313–318.
Napier, J.R., 1993. Hands. Princeton University Press, Princeton, NJ.
Patel, B.A., 2010. The interplay between speed, kinetics, and hand postures during primate terrestrial locomotion. Am. J. Phys. Anthropol. 141, 222–234.
Patel, B.A., Wunderlich, R., 2010. Dynamic pressure patterns in the hands of olive baboons (*Papio anubis*) during terrestrial locomotion: implications for cercopithecoid hand morphology. Anat. Rec. 293, 710–718.
Pontzer, H., Lieberman, D.E., Momin, E., Devlin, M.J., Pok, J.D., Hallgrímsson, B., Cooper, D.M.L., 2006. Trabecular bone in the bird knee responds with high sensitivity to changes in load orientation. J. Exp. Biol. 209, 57–65.
Preuschoft, H., 1973. Functional anatomy of the upper extremity. In: Bourne, G.H. (Ed.), The Chimpanzee. Karger, Basel, pp. 34–120.
Puymerail, L., 2013. The functionally-related signatures characterizing the endostructural organisation of the femoral shaft in modern humans and chimpanzee. C.R. Palevol. 12, 223–231.
R Core Team, 2016. R: a language and environment for statistical computing. R Foundation for Statistical Computing, Vienna.
Rafferty, K.L., 1998. Structural design of the femoral neck in primates. J. Hum. Evol. 34, 361–383.
Richmond, B.G., 2003. Early hominin locomotion and the ontogeny of phalangeal curvature in primates. Am. J. Phys. Anthropol. Suppl. 36, 178–179 (abstract).
Richmond, B.G., 2007. Biomechanics of phalangeal curvature. J. Hum. Evol. 53, 678–690.
Richmond, B.G., Hatala, K.G., 2013. Origin and evolution of human postcranial anatomy. In: Begun, D.R. (Ed.), A Companion to paleoanthropology. Blackwell Publishing Ltd, Malden, pp. 183–202.
Richmond, B.G., Strait, D.S., 2000. Evidence that humans evolved from a knuckle-walking ancestor. Nature 404, 382–385.
Richmond, B.G., Roach, N.T., Ostrofsky, K.R., 2016. Evolution of the early hominin hand. In: Kivell, T.L., Lemelin, P., Richmond, B.G., Schmitt, D. (Eds.), The Evolution of the Primate Hand: Anatomical, Developmental, Functional, and Paleontological Evidence. Springer-Verlag, New York.
Roach, N.T., Lieberman, D.E., 2014. Upper body contributions to power generation during rapid, overhand throwing in humans. J. Exp. Biol. 217, 2139–2149.
Roach, N.T., Venkadesan, M., Rainbow, M.J., Lieberman, D.E., 2013. Elastic energy storage in the shoulder and the evolution of high-speed throwing in *Homo*. Nature 498, 483–486.
Rolian, C., Lieberman, D.E., Zermeno, J.P., 2011. Hand biomechanics during simulated stone tool use. J. Hum. Evol. 61, 26–41.
Rubin, C.T., Lanyon, L.E., 1982. Limb mechanics as a function of speed and gait: a study of functional strains in the radius and tibia of horse and dog. J. Exp. Biol. 101, 187–211.
Ruff, C.B., Trinkaus, E., Walker, A.C., Larsen, C.S., 1993. Postcranial robusticity in *Homo*. I: temporal trends and mechanical interpretation. Am. J. Phys. Anthropol. 91, 21–53.
Ruff, C.B., Holt, B., Trinkaus, E., 2006. Who's afraid of the big bad Wolff?: "Wollfs Law" and bone functional adaptation. Am. J. Phys. Anthropol. 129, 484–498.
Ruff, C.B., Holt, B., Niskanen, M., Sladek, V., Berner, M., Garofalo, E., Garvin, H.M., Hora, M., Junno, J.-A., Schuplerova, E., Vilkama, R., Whittey, E., 2015. Gradual decline in mobility with the adoption of food production in Europe. Proc. Natl. Acad. Sci. U.S.A. 112, 7147–7152.
Runestad, J.A., 1997. Postcranial adaptations for climbing in loridae (Primates). J. Zool. 242, 261–290.
Ryan, T.M., Ketcham, R.A., 2002. The three-dimensional structure of trabecular bone in the femoral head of strepsirrhine primates. J. Hum. Evol. 43, 1–26.
Ryan, T.M., Ketcham, R.A., 2005. Angular orientation of trabecular bone in the femoral head and its relationship to hip joint loads in leaping primates. J. Morphol. 265, 249–263.
Ryan, T.M., Krovitz, G.E., 2006. Trabecular bone ontogeny in the human proximal femur. J. Hum. Evol. 51, 591–602.
Ryan, T.M., Shaw, C.N., 2015. Gracility of the modern *Homo sapiens* skeleton is the result of decreased biomechanical loading. Proc. Natl. Acad. Sci. U.S.A. 112, 372–377.
Ryan, T.M., Walker, A., 2010. Trabecular bone structure in the humeral and femoral heads of anthropoid primates. Anat. Rec. 293, 719–729.
Sakata, T., Sakai, A., Tsurukami, H., Okimoto, N., Okazaki, Y., Ikeda, S., Norimura, T., Nakamura, T., 1999. Trabecular bone turnover and bone marrow cell development in tail-suspended mice. J. Bone Miner. Res. 14, 1596–1604.
Saparin, P., Scherf, H., Hublin, J.-J., Fratzl, P., Weinkamer, R., 2011. Structural adaptation of trabecular bone revealed by position resolved analysis of proximal femora of different primates. Anat. Rec. 294, 55–67.
Sarmiento, E.E., 1988. Anatomy of the hominoid wrist joint: Its evolutionary and functional implications. Int. J. Primatol. 9, 281–345.
Scherf, H., Tilgner, R., 2009. A new high resolution-CT segmentation method for trabecular bone architectural analysis. Am. J. Phys. Anthropol. 140, 39–51.
Schmitt, D., 2003. Insights into the evolution of human bipedalism from experimental studies of humans and other primates. J. Exp. Biol. 206, 1437–1448.
Shaw, C.N., Ryan, T.M., 2012. Does skeletal anatomy reflect adaptation to locomotor patterns? Cortical and trabecular architecture in human and nonhuman anthropoids. Am. J. Phys. Anthropol. 147, 187–204.
Shaw, C.N., Stock, J.T., 2009. Intensity, repetitiveness, and directionality of habitual adolescent mobility patterns influence the tibial diaphysis morphology of athletes. Am. J. Phys. Anthropol. 140, 149–159.
Skinner, M.M., Stephens, N.B., Tsegai, Z.J., Foote, A.C., Nguyen, N.H., Gross, T., Pahr, D.H., Hublin, J.-J., Kivell, T.L., 2015. Human-like hand use in *Australopithecus africanus*. Science 347, 395–399.
Spoor, F., Wood, B.A., Zonneved, F., 1994. Implications of early hominid labyrinthine morphology for evolution of human bipedal locomotion. Nature 369, 645–648.
Stern, J.T.J., 2000. Climbing to the top: a personal memoire of *Australopithecus afarensis*. Evol. Anthropol. 9, 113–133.
Stern, J.T.J., Susman, R.L., 1983. The locomotor anatomy of *Australopithecus afarensis*. Am. J. Phys. Anthropol. 60, 279–317.
Stock, J., Pfeiffer, S., 2001. Linking structural variability in long bone diaphyses to habitual behaviors: foragers from the southern African later

Stone Age and the Andaman islands. Am. J. Phys. Anthropol. 115, 337–348.
Su, A., Wallace, I.J., Nakatsukasa, M., 2013. Trabecular bone anisotropy and orientation in an Early Pleistocene hominin talus from East Turkana, Kenya. J. Hum. Evol. 64, 667–677.
Susman, R.L., 1998. Hand function and tool behavior in early hominids. J. Hum. Evol. 35, 23–46.
Susman, R.L., Stern, J.T.J., Jungers, W.L., 1984. Arboreality and bipedality in the Hadar hominids. Folia Primatol. 43, 283–306.
Thorpe, S.K., Crompton, R.H., 2006. Orangutan positional behavior and the nature of arboreal locomotion in Hominoidea. Am. J. Phys. Anthropol. 131, 384–401.
Trinkaus, E., Ruff, C.B., 1989a. Diaphyseal cross-sectional morphology and biomechanics of the Fond-de-Foret 1 femur and the Spy 2 femur and tibia. Bull. Soc. R. Belge Anthropol. Prehist. 100, 33–42.
Trinkaus, E., Ruff, C.B., 1989b. Cross-sectional geometry of Neandertal femoral and tibial diaphyses: implications for locomotion. Am. J. Phys. Anthropol. 78, 315–316.
Trussell, H.J., 1979. Comments on "Picture thresholding using an iterative selection method". IEEE Trans. Syst. Man Cybern. SMC-9, 311.
Tsegai, Z.J., Kivell, T.L., Gross, T., Nguyen, N.H., Pahr, D.H., Smaers, J.B., Skinner, M.M., 2013. Trabecular bone structure correlates with hand posture and use in hominoids. PLoS One 8, e78781.
Tuttle, R.H., 1967. Knuckle-walking and the evolution of hominoid hands. Am. J. Phys. Anthropol. 26, 171–206.
Ward, C.V., 2002. Interpreting the posture and locomotion of *Australopithecus afarensis*: where do we stand? Am. J. Phys. Anthropol. 35, 185–215.
Ward, C.V., Kimbel, W.H., Johanson, D.C., 2011. Complete fourth metatarsal and arches in the foot of *Australopithecus afarensis*. Science 331, 750–753.
Whitehead, P.F., 1993. Aspects of the anthropoid wrist and hand. In: Gebo, D.L. (Ed.), Postcranial Adaptation in Nonhuman Primates. Northern Illinois University Press, DeKalb, IL, USA, pp. 96–120.
Williams, E.M., Gordon, A.D., Richmond, B.G., 2012. Hand pressure distribution during Oldowan stone tool production. J. Hum. Evol. 62, 520–532.
Williams, E.M., Gordon, A.D., Richmond, B.G., 2014. Biomechanical strategies for accuracy and force generation during stone tool production. J. Hum. Evol. 72, 52–63.
Wunderlich, R.E., Jungers, W.L., 2009. Manual pressures during knuckle-walking in chimpanzees (*Pan troglodytes*). Am. J. Phys. Anthropol. 139, 394–403.
Zeininger, A., Patel, B.A., Zipfel, B., Carlson, K.J., 2016. Trabecular architecture in the StW 352 fossil hominin calcaneus. J. Hum. Evol. 97, 145–158.
Zeininger, A., Richmond, B.G., Hartman, G., 2011. Metacarpal head biomechanics: a comparative backscattered electron image analysis of trabecular bone mineral density in *Pan troglodytes*, *Pongo pygmaeus*, and *Homo sapiens*. J. Hum. Evol. 60, 703–710.